2019 IEEE 4th International Conference on Advanced
Robotics and Mechatronics (ICARM)

Development of A Parallel-elastic Robot Leg for Loaded Jumping

Zewen He[1], Fei Meng[12], Xuxiao Fan[12], Ru Kang[1], Shengkai Liu[1], Huaxin Liu[12], Zhangguo Yu[12], Mingyue Qin[1], Aiguo Ming[23] and Qiang Huang[12]

***Abstract*— Legged robot in middle-large size has limited capacity in jumping especially when loaded in practical situation. Parallel elasticity in motor-driven joint has a primary advantage that the spring force will help to increase resultant torque exceeding the motor's performance limitation, which serial elasticity does not. To achieve good performance for jumping motion, we design a novel parallel elastic robot leg, which could realize loaded high jump. Structure of the robot leg uses parallel four-bar mechanism equipped with a tension spring across two hinge points, which is a pattern of Parallel Elastic Actuation (PEA). In this paper, a simplified principle model is constructed to analyze robot dynamics, and simulate the motion trajectory for a maximum-height jump. Then, several hardware principles are followed in robot design conforming to spring-mass model. Moreover, a prototype of the parallel leg is developed, on which the loaded vertical jump experiments are achieved. The results of experiment validate the ability in loaded jumping of the robot leg, which could implement a vertical loaded jump in maximum jumping height of 30cm (total mass 6.5kg, spring stiffness 225N/m) and 33cm (10kg, 450N/m).**

I. Introduction

Jumping as a necessary skill for most legged animals, plays an important role in preying and escaping behavior. Mammals as antelope and deer though with heavy body, still have an excellent jumping ability in nature. In biomimetic robotics, on one hand large-size robots have been developed for various functions that act like real animal, while jumping capacity is still a weakness, while on the other hand recent researches about jumping motion are more focus on tiny robots. As in some researches, smaller animals need a higher angular speed on joint to realize a similar maximal height [1]. Actually larger and heavier animals should reach a much higher joint torque to achieve the similar high jump with their big-weight trunk. This explains why jumping especially loaded jumping is challenging for medium and large robot. In general, actuator power is the critical limitation of maximum jumping height.

To reduce the actuator inertia and transmission dissipation, direct drive (DD) and quasi-direct drive (QDD) became popular in small robot like Minitaur [2], GOAT [3] and Ding's work [4]. However, as the robot size and mass grow, the low-ratio actuator has excessively harsh condition of motor torque and power for the similar magnitude of jump. In order to realize feasible loaded jump on larger robot, available peak power is necessary in the motion process. In [5], a behavior named power modulation was introduced as a method of jumping power amplification. In practical application, appropriately mechanical elasticity is effective implementation of power modulation. Comparing with virtual compliance, mechanical spring system avoids the potential problem about actuator bandwidth and inefficiency of electrical regeneration [6]. SEA and PEA are two types of fundamental mechanical elastic elements, which are inspired by Hill-type model in muscle issue [7]. Both SEA and PEA can assist the actuator in improving jumping performance. The primary advantage of SEA is that the actuator inertia is coupled by spring to joint inertia, so the motor is isolated from impact and the actuator inertia does not interfere with joint motion [8]. ATRIAS [6] and ScarlETH [9] used plate spring and pre-compressed linear spring as serial-elastic element respectively, achieving passive compliance in dynamical motion. Another feature of SEA is the ability of energy storing and adaptability to high-frequency motion like hopping or bounding [5]. Sugoi Neco from UEC, utilized Elastic Four-bar Linkage Mechanism (can be seen as serial elasticity) mimicking animal's tendon, and validated the assistance of serial elastic element in high jump and soft landing [10]. Conversely, in PEA the motor torque and spring force act additively [8], which reduce the required peak power of actuator notably; furthermore, PEA can increase the energetic storage in the air [5]. Robot Phides [11] and ERNIE [12] are examples that used PEA in knee joint, confirming the function in reduction of necessary torque and power. Though the price is that PEA will consume extra energy for pre-loading (crouching motion before jump) [13], and has lower efficiency than SEA [14], equipment of parallel spring is still the reasonable choice to amplify the sum power of the actuator in loaded jumping.

The main purpose of our work is to design a mechanically reliable robot leg with parallel elastic structure, realizing high jump and loaded high jump in practice and fitting the property of motor with the help of parallel spring. The robot prototype we developed consists of two high-power motors with harmonic reducer, four light carbon fiber tubes and required sensors. Hardware configurations of the prototype are determined following the principles as high torque density of motor, high transparency of actuator, light leg material and proper elasticity of foot end. In simulation, optimization of jumping motion for maximum height was executed based on

The corresponding author is Fei Meng, email: mfly0208@bit.edu.cn

This work was supported by the National Natural Science Foundation of China under Grants 61703044, 91748202, 61673069.

[1]Intelligent Robotics Institute, School of Mechatronical Engineering, Beijing Institute of Technology, 5 Nandajie, Zhongguancun, Haidian, Beijing, 100081, China

[2]Beijing Advanced Innovation Center for Intelligent Robots and Systems, Beijing Institute of Technology, Beijing, China

[3]Department of Mechanical Engineering and Intelligent Systems, The University of Electro-Communications, Tokyo, Japan

978-1-7281-0064-7/19/$31.00 ©2019 IEEE

Authorized licensed use limited to: Mohamed bin Zayed University of Artificial Intelligence. Downloaded on August 12,2026 at 13:54:53 UTC from IEEE Xplore. Restrictions apply.

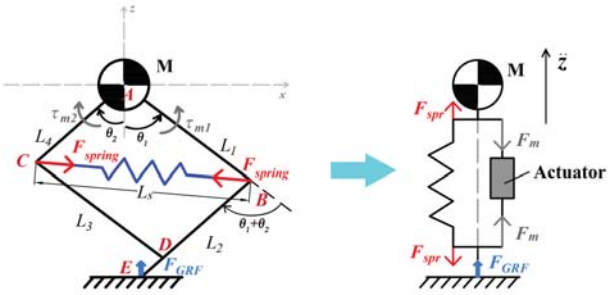


Fig. 1. Schematic of parallel four-bar linkage mechanism with diagonal spring (left); equivalent PEA model (right). A to E are hinge points, L_s is length of tension spring, M is mass of the body, and θ_i is joint angle. F_{spr} and F_m are equivalent force of spring and motor torque.

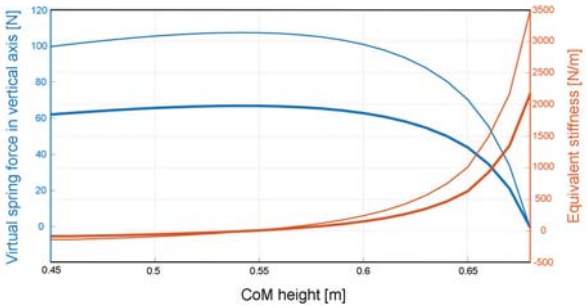


Fig. 2. Virtual spring force F_{spr} and equivalent stiffness ($k_{vir} = \frac{dF_{spr}}{d\lambda}$, λ is the compressed displacement of leg length) of the spring system in vertical direction: blue represents spring force, and orange represents stiffness; thick and thin curves mean K=255N/m and 410N/m respectively.

a simplified model according to parallel-elastic mechanism. As in vertical jump experiment, the robot leg can realize the high jump in two loaded condition with different elastic configuration, which proved the feasibility of our parallel robot leg. The rest parts of the paper are arranged as follows. In Section II, dynamic analysis of principle model and selection of structural parameter are introduced. Section III describes the design of actuator and robot prototype. Section IV shows the experiments and Section V is conclusion.

II. Model Analysis and Structural Configuration

A. Fundamental model analysis

The basic mechanism of our robot leg is a parallel four-bar linkage mechanism articulated on robot trunk. In the schematic model shown in Fig. 1(a), the whole mass of leg is lumped at Point A, and the mass-less linkages L_1 to L_4 construct the parallel mechanism(in length: L_1 = L_3 and L_2 = L_4). As linkage L_1 and L_4 can rotate around Joint A, the model has two DOFs to realize planar motion. Forward kinematics of this model are calculated in Appendix. The diagonal spring along the line segment BC is linear, and the tensile force of the spring is deduced by: $F_{spring} = k \cdot (l - l_{ini})$, where l_{ini} is the initial length of diagonal spring and l is the actual length of the spring (calculation of l shown in Appendix).

Fig. 1(a) also displays the force condition of the parallel leg. In vertical direction, the parallel leg with motor torque and diagonal spring effects can be regarded as a spring-mass model with parallel nonlinear spring and actuator, shown in Fig. 1(b). In this schematic, the entire mechanism with origin diagonal spring is converted into a virtual vertical spring connected with a mass point. F_{spr} is elastic force of virtual spring, F_m the external force generated by motor torque effects on both ends of spring, and F_{GRF} the ground reaction force on the bottom. Due to the virtual spring is massless, the forces on its two ends are equal. On the bottom end, there is a force equation:

$$F_{GRF} = F_{spr} - F_m \tag{1}$$

Transformational relation between joint torque and force on endpoint is given by: $\boldsymbol{\tau = J^T F}$,where $\boldsymbol{J}$ is the Jacobian matrix derived in Appendix. Therefore, (1) can be transformed as:

$$\boldsymbol{\tau_{GRF} = \tau_{spr} - \tau_m} \tag{2}$$

$\boldsymbol{\tau_m}$ is motor torque in Fig. 1(a); $\boldsymbol{\tau_{GRF}}$ and $\boldsymbol{\tau_{spr}}$ are corresponding torques to forces in (1) on each joints. Theoretically, torque of diagonal spring can be obtained by using virtual work principle as in (3).

$$\boldsymbol{F_{spring} \cdot \delta l = \tau_{spr} \cdot \delta \theta} \tag{3}$$

where, $\delta \boldsymbol{l}$ and $\delta \boldsymbol{\theta}$ are virtual displacement of spring end and joint angle respectively, and $\boldsymbol{F_{spring}}$ is spring tension shown in Fig. 1(a). Substituting Equations(2)(3) into (1), F_{GRF} can be deduced, and vertical acceleration of the mass point can be derived as:

$$\ddot{z} = \frac{F_{GRF}}{M} - g \tag{4}$$

where, $\ddot{z}$ is the acceleration in z-axis and M is the total mass of the model.

Obviously, in vertical direction, the effect of diagonal spring counteracts part of gravity. Thus, parallel-elastic mechanism improves the performance of vertical high jump motion by providing an additional torque on the two active joints. Correspondingly, the spring generates the same torque while impedes the motion when pull back the leg, which leads to an inefficiency in reverse movement.

B. Structural parameter optimization

To obtain an appropriate configuration of the mechanism, the method of selecting linkage length and spring parameter has been discussed.

1) Leg length optimization: Focusing on vertical jump motion, we pay more attention to motion range of leg in vertical direction. Thus, in order to maximize vertical workspace (radius difference between legs minimum and maximum extension) in takeoff motion, an optimization of the linkage length is proposed.

Authorized licensed use limited to: Mohamed bin Zayed University of Artificial Intelligence. Downloaded on August 12,2026 at 13:54:53 UTC from IEEE Xplore. Restrictions apply.

In the aspect of body size, the prospective design of our robot is mimicking large quadruped animal like antelope, therefore the sum length of the two linkages is set as 0.7m, which is also close to some classic middle-size robots such as Spotmini and MIT Cheetah. The goal of the optimization is finding the best ratio of L_1 and L_2 to achieve the largest vertical foot-end coverage. In the result, we found that in condition of $L_1 = L_2$ the foot end could obtain the maximum motion radius, and L_1 = 0.35m, L_2 = 0.35m are set as the optimal length. After optimizing L_1 and L_2, we further determine $L_3 = L_1$ in the parallel model, and L_4 = 0.285m for some structural reasons.

2) Spring stiffness determination: As mentioned in Section II.A, the spring force effects on both directions of leg movement, hence there is a contradiction in seeking proper stiffness of the parallel spring for vertical jump. For practical reasons, several principles are summarized to select spring stiffness: firstly, the vertical support force generated by spring should be greater than the gravity of whole leg in standing phase; secondly, the parallel spring cannot be too large to make the robot leg difficult and inefficient to crouch. In our analysis, vertical virtual force of diagonal spring (F_{spr} in Fig. 1(b)) is a nonlinear function of leg length (as in Fig. 2), and its value is an approximate constant when leg length is less than 0.63m. Therefore, we assume that the condition of spring stiffness selection is that the virtual spring force F_{spr} can just support robot's gravity without active motor torque in leg's minimum length (0.45m in practice). After setting the total weight of robot leg, we can use the linkage parameter determined in Section II.A to calculate the spring force F_{spr} and deduce the optimal stiffness of diagonal spring. In following experiments, the prototype is arranged to jump in two cases that the total mass is 6.5kg or 10kg; thus the optimal spring stiffness in the experiments are 255N/m and 410N/m respectively, and the virtual spring force and equivalent stiffness are shown in Fig. 2. For engineering reasons, we choose the standard spring LE-085JK-08, whose original length is 0.165m, extreme length 0.538m, and stiffness coefficient 225N/m. In the experiments, we can change the total stiffness of the mechanism by adding or subtracting the spring's number.

In Fig. 2, different from serial chain mechanism, parallel mechanism with diagonal spring has some special features. Vertically virtual force of the spring system increases gently as the CoM rises, and a peak value appears in the springs middle length; finally the force curve declines rapidly. This feature illustrates that the diagonal spring provides an almost constant force on the robot trunk in the beginning of jump, and reduces to zero at the end of the process. In this case, the parallel spring could be regarded as an assistor in vertical jump, while should be pre-loaded in leg's maximum length.

III. Hardware Design

A. Actuator

In the sketch model, there are two DoFs in the leg, so two motors are necessary to control robot's movement. Refer to force analysis, two active joints provide similar torques in vertical motion. Thus, we design the same actuator for both joints. In jumping locomotion, actuators will reach the maximal torque and speed in the same time [4], therefore in some research [15] torque density and maximum rotational speed are both principal consideration for motor selection. Hence the power density is the appropriate measurement of the motor. Besides, reduction ratio decides the balance between joint torque and speed. The higher the reduction ratio, the bigger the output torque and the lower speed, while high ratio reducer may cause big rotational inertia and decrease the transparency of the actuator.

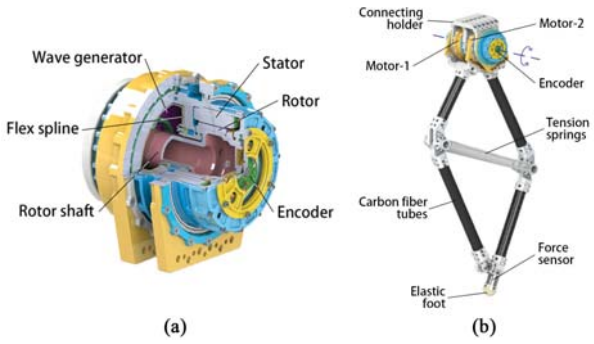


Fig. 3. (a) Cross-section view of the actuation module, containing motor and harmonic reducer; (b) mechanical configuration of robot leg.

In estimation, one leg need to support 5.2kg for its own weight and almost 10kg in sum when assembled on quadruped robot. Actuators should generate enough torque and speed at the same time, satisfying the loading demand and realizing high-speed movement in jumping process. Taking these into account, we select a self-developed motor as joint motor and reducer (reduction ratio 31:1) in the actuator. Power density of the motor is 808.82W/kg, which is the top level in the same specification. Structure of actuation design is exhibited in Fig. 3.

B. Leg mechanism design

According to previous research, motor mass should take large portion in the robot's mass budget [16]. Based on this notion, we utilize the light material on leg bars and connections. Consequently, carbon fiber tube is used as leg linkage, and joint connections are made of aluminum. Mass of the total robot leg is 5.2kg while motor module weighs 3.04kg in sum, so the percentage in total mass taken up by actuator is 58% approximately, which is higher than robot GOAT and Minitaur. Concrete parameter of the robot leg see also Table. I.

Fig. 3(b) presents the 3D structural design. In the figure, the whole leg can be installed on the robot trunk or other planar. Carbon fiber tube is connected with motor shaft by a U-type linkage. A tension spring is hung between two middle joints, which coincides diagonal line of the parallel structure. A force sensor is fixed on the bottom joint, and a polyurethane block is connected on the other end of the sensor to mitigate impact as a serial elastic element in landing passively. It's worth noting that the foot end is not on the

978-1-7281-0064-7/19/$31.00 ©2019 IEEE

Authorized licensed use limited to: Mohamed bin Zayed University of Artificial Intelligence. Downloaded on August 12,2026 at 13:54:53 UTC from IEEE Xplore. Restrictions apply.

TABLE I
PARAMETERS OF ROBOT LEG

Part name		Length [m]	Mass [kg]
Linkage (containing joint connections)	L_1	0.35	0.23
	L_2	0.35	0.23
	L_3	0.35	0.23
	L_4	0.285	0.19
Tension spring		0.165∼0.538	0.13
Force sensor		0.06	0.26
Motor module (single)		/	1.52
Connecting holder		/	0.45

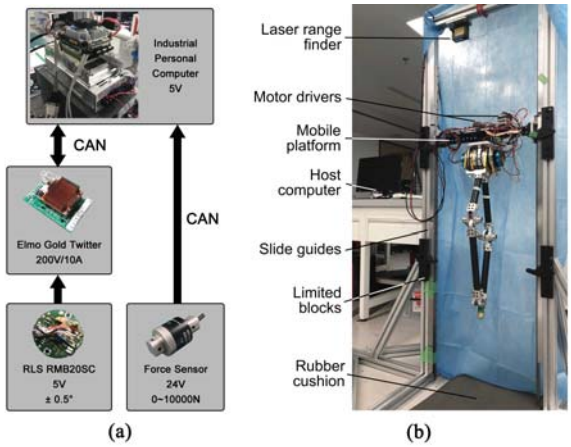


Fig. 4. (a) Diagram of control system; (b) experimental setup of robot prototype.

extension line of two joints, so a modified model for our robot is shown in Fig. 5(b). Point E in this figure is in a different position with which in Fig. 1 observably. The angle range of linkage L_1 and L_2 (θ_1 and θ_2 in Fig. 5(b)) is -70∼100° symmetrically.

C. Control system and sensors

Control system of our robot consists of Industrial Personal Computer (IPC) as upper computer to execute real-time planning and information processing, and Elmo Motor Driver as lower controller to support underlying position control on motors. Between IPC and drivers, we adopt CAN bus as transmission mode. On motor, 12-bit magnetic encoder is used to record motor angle. On the foot of the robot, force sensor is installed to gather force signal and send it to upper computer by CAN bus. Fig. 4 (a) demonstrates the structure of control system. Control period of our system is set as 2ms in experiment.

IV. EXPERIMENTS

To validate feasibility of torque control and loaded jump ability of our robot prototype, a series of experiments are conducted. Fig. 4 depicts the experimental setup: the whole leg is fixed on an aluminum platform that can only move vertically between two slide guides. The linear guides and a laser range finder are installed on a supporting frame. Weights are fixed on mobile platform to adjust the total mass of the robot in different cases.

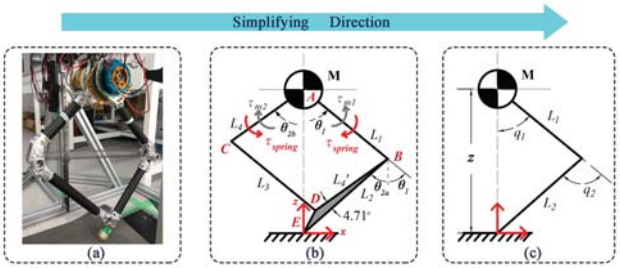


Fig. 5. (a) Robot leg prototype; (b) detailed model including the same kinematics as prototype; (c) simplified knee extensor model. In (b), θ_{2b}=θ_{2a}+4.71°; in (c), angle q_1 is equal with θ_{2a} in (b).

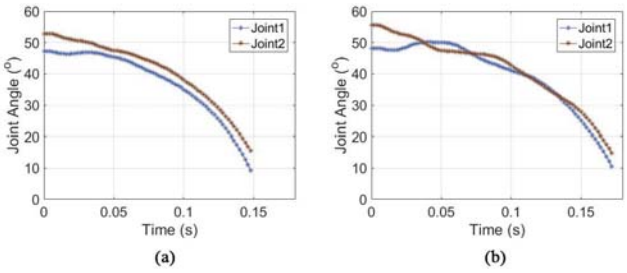


Fig. 6. Joint angle curves of θ_1 and θ_2 during takeoff process in two configurations. (a) 6.5kg, 225N/m; (b) 10kg, 450N/m.

A. Preliminary experiment

To realize torque control using motor driver, we completed static calibration experiment on the actuators. A simple device with spring dynamometer was designed to measure the output torque of the actuator, and real-time input current was recorded by Elmo driver. After several groups of data obtained, a fitting function was used to describe the relationship between current and torque. In the result, there is a linear function: τ=$a \cdot I + b$, where τ is actuator torque, I is motor current and a, b are coefficients. In Joint1, a is 4.82, and b is -3.59, while in Joint2, a 4.50, b -2.16.

B. Vertical jump experiment

In order to seek the ultimate ability of our robot leg in loaded high jump with given hardware configuration, a nonlinear optimization problem is formulated. To simplify the dynamic analysis, the entire robot can be abstracted as a two-link knee extensor model [4]. Fig. 5 shows the simplifying

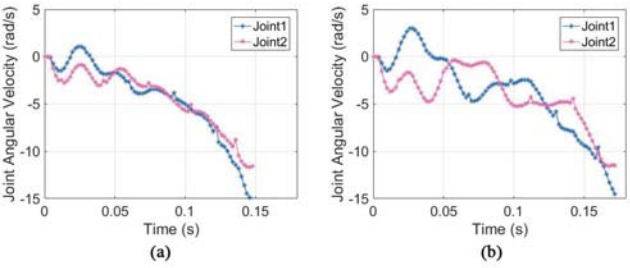


Fig. 7. Joint angular velocity of θ_1 and θ_2 during takeoff process in two configurations. (a) 6.5kg, 225N/m; (b) 10kg, 450N/m.

Authorized licensed use limited to: Mohamed bin Zayed University of Artificial Intelligence. Downloaded on August 12,2026 at 13:54:53 UTC from IEEE Xplore. Restrictions apply.

process of the robot. Fig. 5(b) is the abstract model of prototype in (a), and (c) is the two-link model equivalent with (b) in kinematics. In two-link model, all mass is lumped at the base, which is on the motor axis. The base only moves in the z-axis on its foothold, and the foothold is assumed as fixed on the floor in stance phase. Force analysis of model in (b) and (c) is familiar with what in Section II.A, but need to note that angle q_2 in (c) is not equal with θ_2 in Fig. 1. All the external force and torque can be transformed into resultant force on mass point.

In optimization, we set joint torque τ_1 and τ_2 as the variables to find maximum jumping height as optimal goal. 4^{th} order B-spline curve defined from several knots and control points is introduced to describe the joint torque trajectories: $\boldsymbol{t} := [0;0;0;t_1;t_2;t_3;T_{end};T_{end};T_{end}]$, $\boldsymbol{\tau} := [\tau_1;\tau_2;\tau_3;\tau_4;0]$, where T_{end} represents the end time of the simulation. t_i(i=1∼3) and τ_j(j=1∼4) are optimization variables which satisfy $t_i \leq T_{end}$ and $|\tau_j| \leq \tau_{\max}$ ($\tau_{\max}$ is the maximum output torque of actuator in estimation). Jump motion will start in a relatively extreme posture ($\theta_1 = \theta_2 = 50°$) to simplify the optimization problem, and initial height of CoM this moment is 0.45m.

In each round of simulation, with the original torque curves as input, a rough motor model is constructed to constrain the torque input according to specific torque-speed curve of given actuator. The leg model will take off when: $z_t \geq z_m$, where z_t is real-time height of CoM which is deduced by double integrating $\ddot{z}$ in (4), and z_m the feasible height in stance phase (is also the extreme leg length, here is set as 0.65m). Maximum jumping height can be expressed as: $h_{\max} = z_t + \frac{\dot{z}_t^2}{2g}$. The overall simulation above is constructed in MATLAB Simulink that step time is set as 0.0001s, and nonlinear optimization has been performed using MATLAB $fmincon$ function; and the objective function of this problem is: $-h_{max}$.

In actual measurement, the whole legged robot with its guide device weighs about 6.5kg. In the future work of quadruped robot, each leg have to bear 10kg in total at least (including its own weight). According to the conditions above, we set jumping simulation and experiment in 3×2 cases: robot equipped with no spring (total stiffness: K=0N/m), one spring (K=225N/m) or two springs (K=450N/m) when no-loaded (total mass=6.5kg) or loaded (mass=10kg) respectively. After obtaining the optimal joint torque trajectories in simulation, we put them into robot prototype to observe practical result.

Experiment results in all 6 cases are shown in Table. I. The jumping heights in the table are relatively vertical displacement of motor axis from liftoff moment (liftoff moment here is in the leg's unbending length, i.e. 0.65m) to its highest point. Fig. 6 to Fig. 8 depict angle curve, angular velocity, joint torque and joint power in two cases respectively. Fig. 9 shows the snapshots of the jumping in the case: 10kg & K=450N/m.

TABLE II
RESULT OF LOADED JUMPING EXPERIMENTS

	non-spring	1 spring (225N/m)	2 spring (450N/m)
6.5kg	23cm	30cm	/*
10kg	18cm	23cm	33cm

* In this case spring torque is so large that the robot leg cannot crouch down naturally.

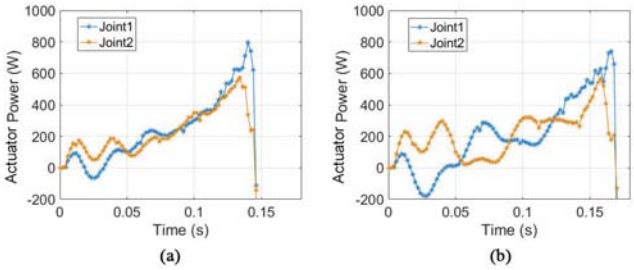


Fig. 8. Actuator power of Joint1 and Joint2 during takeoff process in two configurations. (a) 6.5kg, 225N/m; (b) 10kg, 450N/m.

C. Discussion

Theoretically, jumping robot need high torque in the beginning, while high velocity at the end of the motion [17]. In practical terms, actuator starts up with zero-torque and zero-velocity, and as in (5), the determining factor of jumping height is the position and velocity at take-off moment. While extreme extension length of the leg is decided by mechanical structure, and limiting velocity is constrained by the actuator capacity, key point of the motion trajectory is the acceleration process in stance phase.

In simulation, all the torque-speed curves tend to the limiting curve at the end of motion. While the mechanical stroke in stance phase is limited, experiments with no or low elasticity cannot reach the maximum speed of actuator during the process, validating the effect of parallel spring in loaded jump.

As in the experiment results, the robot leg realized loaded high jump with the help of diagonal spring (jumping process video see annex). While compared with the simulation results, the maximum height is relatively smaller because of the mechanical loss of robot prototype. In Table. I, we found that in 6.5kg/1-spring and 10kg/2-spring situations, the robot can reach the similarly maximum heights; while in the same mass situation with lower elasticity, the robot jumps lower. It is worth mentioning that data in 6.5kg/2-spring situation was ignored, due to the overlarge spring stiffness limiting the crouch-down movement of the leg, which is extremely inefficient in practical application. In Fig. 6, angle trajectories in two different cases reveal considerable similarity, while in 10kg situation the motion takes longer time. In Fig. 7 and Fig. 8, it can be seen that the maximum angular velocity and power value in two cases are very close, and reach the actuator's ultimate property. In these two cases the robot was loaded in different weight, but reveal the similar performance. The results above prove that the diagonal spring increases the resultant torque of each joint,

Authorized licensed use limited to: Mohamed bin Zayed University of Artificial Intelligence. Downloaded on August 12,2026 at 13:54:53 UTC from IEEE Xplore. Restrictions apply.

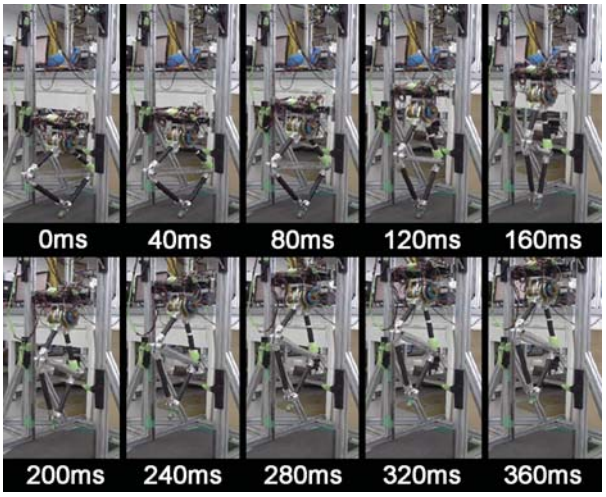


Fig. 9. Snapshots of the jumping motion in the case: K=450N/m, 10kg in total. The robot jumps 33cm in the last picture (displacement from lift-off to the peak height.

and offsets gravity in vertical direction observably, validating correctness of the design method in Section II.B. Therefore, the parallel structure with diagonal spring is feasible in loaded jump, and suitable for performance-known actuators.

V. Conclusion and Outlook

This paper introduces a parallel robot leg equipped with diagonal spring for loaded jumping motion. The spring as a parallel elastic element increases the resultant torque on joint for high jump. Consequently, with the optimization of hardware configuration and motion planning, the robot prototype achieved high jump of 30cm (6.5kg, 225N/m) and 33cm (10kg, 450N/m), which validated the key role that diagonal spring played in loaded jump and illustrated the practical significance in multiple potential applications.

In the future work, more different tasks will be accomplished by the robot leg. Furthermore, a quadruped robot with four parallel legs will be designed to implement quadruped jumping motion.

Appendix

Given two joint angles θ_1 and θ_2, as in Fig. 1, foot end position of this model is:

$$\begin{cases} x_{toe} = L_1 \cdot \sin\theta_1 - L_2 \cdot \sin\theta_2 \\ z_{toe} = -L_1 \cdot \cos\theta_1 - L_2 \cdot \cos\theta_2 \end{cases} \tag{5}$$

where, x_{toe} and z_{toe} are the coordinates of toe (Point E). Based on this, the Jacobian matrix of the leg mechanism can be solved as:

$$J = \begin{bmatrix} L_1 \cdot \cos\theta_1 & -L_2 \cdot \cos\theta_2 \\ L_1 \cdot \sin\theta_1 & L_2 \cdot \sin\theta_2 \end{bmatrix} \tag{6}$$

Then the distance between Joint B and Joint C, which is the actual length of diagonal spring, has a deduction as in (7).

$$l^2 = (L_4 \sin\theta_2 + L_1 \sin\theta_1)^2 + (L_4 \cos\theta_2 - L_1 \cos\theta_1)^2 \tag{7}$$

References

[1] K. Schmidt-Nielsen, *Scaling: why is animal size so important?* Cambridge university press, 1984.
[2] G. Kenneally, A. De, and D. E. Koditschek, "Design principles for a family of direct-drive legged robots," *IEEE Robotics and Automation Letters*, vol. 1, no. 2, pp. 900–907, 2016.
[3] S. Kalouche, "Goat: A legged robot with 3d agility and virtual compliance," in *2017 IEEE/RSJ International Conference on Intelligent Robots and Systems (IROS)*. IEEE, 2017, pp. 4110–4117.
[4] Y. Ding and H.-W. Park, "Design and experimental implementation of a quasi-direct-drive leg for optimized jumping," pp. 300–305, 2017.
[5] D. W. Haldane, M. M. Plecnik, J. K. Yim, and R. S. Fearing, "Robotic vertical jumping agility via series-elastic power modulation," *Science Robotics*, vol. 1, no. 1, 2016.
[6] C. Hubicki, J. Grimes, M. Jones, D. Renjewski, A. Spröwitz, A. Abate, and J. Hurst, "Atrias: Design and validation of a tether-free 3d-capable spring-mass bipedal robot," *The International Journal of Robotics Research*, vol. 35, no. 12, pp. 1497–1521, 2016.
[7] F. E. Zajac, "Muscle and tendon: properties, models, scaling, and application to biomechanics and motor control." *Critical reviews in biomedical engineering*, vol. 17, no. 4, pp. 359–411, 1989.
[8] Y. Yesilevskiy, Z. Gan, and C. D. Remy, "Optimal configuration of series and parallel elasticity in a 2d monoped," in *2016 IEEE International Conference on Robotics and Automation (ICRA)*. IEEE, 2016, pp. 1360–1365.
[9] M. Hutter, C. D. Remy, M. A. Hoepflinger, and R. Siegwart, "Scarleth: Design and control of a planar running robot," in *2011 IEEE/RSJ International Conference on Intelligent Robots and Systems*. IEEE, 2011, pp. 562–567.
[10] R. Sato, I. Miyamoto, K. Sato, A. Ming, and M. Shimojo, "Development of robot legs inspired by bi-articular muscle-tendon complex of cats," in *Proceedings. IEEE/RSJ International Conference on Intelligent Robots and Systems (IROS)*. IEEE, 2015, pp. 1552–1557.
[11] J. D. Karssen, M. Haberland, M. Wisse, and S. Kim, "The effects of swing-leg retraction on running performance: analysis, simulation, and experiment," *Robotica*, vol. 33, no. 10, pp. 2137–2155, 2015.
[12] T. Yang, E. R. Westervelt, J. P. Schmiedeler, and R. A. Bockbrader, "Design and control of a planar bipedal robot ernie with parallel knee compliance," *Autonomous robots*, vol. 25, no. 4, p. 317, 2008.
[13] M. Grimmer, M. Eslamy, S. Gliech, and A. Seyfarth, "A comparison of parallel-and series elastic elements in an actuator for mimicking human ankle joint in walking and running," in *2012 IEEE International Conference on Robotics and Automation*. IEEE, 2012, pp. 2463–2470.
[14] Y. Yesilevskiy, W. Xi, and C. D. Remy, "A comparison of series and parallel elasticity in a monoped hopper," in *2015 IEEE International Conference on Robotics and Automation (ICRA)*. IEEE, 2015, pp. 1036–1041.
[15] S. Seok, A. Wang, D. Otten, and S. Kim, "Actuator design for high force proprioceptive control in fast legged locomotion," in *2012 IEEE/RSJ International Conference on Intelligent Robots and Systems*. IEEE, 2012, pp. 1970–1975.
[16] H. Rad, P. Gregorio, and M. Buehler, "Design, modeling and control of a hopping robot," in *Proceedings of 1993 IEEE/RSJ International Conference on Intelligent Robots and Systems (IROS'93)*, vol. 3. IEEE, 1993, pp. 1778–1785.
[17] M. Okada and Y. Takeda, "Optimal design of nonlinear profile of gear ratio using non-circular gear for jumping robot," in *2012 IEEE International Conference on Robotics and Automation*. IEEE, 2012, pp. 1958–1963.

Authorized licensed use limited to: Mohamed bin Zayed University of Artificial Intelligence. Downloaded on August 12,2026 at 13:54:53 UTC from IEEE Xplore. Restrictions apply.